Received: 31 January 2024 | Revised: 22 March 2024 | Accepted: 25 March 2024

DOI: 10.1002/cjce.25269

SPECIAL ISSUE ARTICLE

THE CANADIAN JOURNAL OF CHEMICAL ENGINEERING

Cohesive particle–fluid systems: An overview of their CFD simulation

Filippo Marchelli[1] | **Luca Fiori**[1] | **Renzo Di Felice**[2]

[1]Department of Civil, Environmental and Mechanical Engineering, University of Trento, Trento, Italy

[2]Department of Civil, Chemical and Environmental Engineering, University of Genova, Genova, Italy

Correspondence
Filippo Marchelli, Department of Civil, Environmental and Mechanical Engineering, University of Trento, Italy.
Email: filippo.marchelli@unitn.it

Funding information
European Commission, Grant/Award Number: E65F21002000007

Abstract

Solid particles may experience different kinds of cohesive forces, which cause them to form agglomerates and affect their flow in multiphase systems. When such systems are simulated through computational fluid dynamics (CFD) programs, appropriate modelling tools must be included to reproduce this feature. In this review, these strategies are addressed for various systems and scales. After an introduction of the different forces (van der Waals, electrostatic, liquid bridge forces, etc.), the modelling approaches are categorized under three methodologies. For diluted slurries of very fine particles, many researchers succeeded with pseudo-single phase approaches, employing a model for the non-Newtonian rheology. This was especially popular for sludges in anaerobic digestions or certain types of soils. In other cases, continuum-based approaches seem to be more adequate, including cohesiveness in the kinetic theory of granular flows or the restitution coefficient. Geldart-A particles experiencing van der Waals forces are the primary focus of such studies. Finally, when each particle is modelled as a discrete element, the cohesive force can be directly specified; this is especially widespread for the wet fluidization case. For each of these approaches, a general overview of the main strategies, achievements, and limits is provided.

KEYWORDS

computational fluid dynamics, discrete element method, granular materials, multiscale modelling, two-fluid method

1 | INTRODUCTION

The word 'cohesion', deriving from the Latin verb 'cohaereo', is defined in the Oxford English Dictionary as 'the action or condition of cohering; cleaving or sticking together'.[1] Despite its many figurative uses, the term identifies the tendency of alike physical elements to be attracted to one another. In this sense, it differs from the word 'adhesion', which instead indicates an attraction towards something different from the subject itself. For example, the cohesiveness among water molecules causes them to coalesce and form drops, while their adhesiveness causes them to adhere to the walls of glass containers, forming a concave meniscus. Although cohesion is often associated with molecules and other microscopic elements, granular materials can also possess such a property.

Granular materials are groups of macroscopic solid particles that primarily interact with each other through contact forces. They are ubiquitous in nature and human activities, but there remain ample knowledge gaps in the fundamental description of the behaviour of these materials,[2] which in 2005 was included by Science authors among noteworthy open research questions.[3] The recent extensive review article by Tahmasebi summarized

many aspects of granular materials, including their characterization.[4] The various knowledge gaps have not stopped humankind from harnessing granular materials in the most diverse fields: grains and flours in the food industry, soils and snow in geophysics and geotechnics, catalysts and heat carriers in chemical engineering, and so forth. The diversity of materials and applications has also favoured the development of various engineering models for these materials, sometimes with a lack of collaboration among different fields. This is especially true for multiphase systems (such as gas–solid or liquid–solid systems) where the presence of a moving fluid phase affects the behaviour of the particles. In chemical engineering, fluidized bed reactors[5] constitute perhaps the best known and studied example of such systems. In these reactors, a bed of solid particles is suspended due to the drag force exerted by an upward-moving fluid, creating a peculiar fluid dynamic regime that is advantageous for various applications.

In engineering applications, modelling tools for such multiphase systems have become irreplaceable thanks to their predictive capabilities and potential to avoid costly experiments. They employ computational fluid dynamics (CFD), employing the numerical solution of the local balance equations of mass, momentum, and energy to provide a detailed description of the unit/phenomenon of interest. Originally developed for single-phase fluid systems, it is nowadays also established for multi-fluid and fluid–solid systems.

Reproducing the trajectory of a single sphere in a fluid is straightforward and, despite some residual uncertainties, systems comprising multiple cohesionless identical spheres are also rather easy to simulate. Any further departure from such a scenario implies much more complexity and less established models. This is the case for the presence of a particle size distribution, of non-spherical particles, of chemical reactions, and of interparticle cohesive forces. Various publications have summarized the modelling approaches for some of these cases. Examples are the works by Zhong et al. for reacting systems,[6] by Ma et al. for non-spherical particles,[7] and by LaMarche et al.[8] and Norouzi et al.[9] for the problems in the estimation of the fluid–solid drag force. Moreover, the very recent reviews by Alobaid et al.[10] and by Wang et al.[11] provide a very extensive resume on the CFD simulation of fluidized beds.

Among the aforementioned non-idealities, cohesiveness plays an important role in different systems and can have diverse causes, most notably van der Waals forces and capillary forces. While the former is most relevant for fine particles and is an intrinsic property, the latter can affect all particle sizes and is caused by the presence of water (or other fluids) among particles. The simulation of cohesive systems has never been reviewed as a whole but rather focusing on single causes of cohesiveness or according to practical applications, such as the works by Xu et al.,[12] Kamphorst et al.[13] and Boyce[14] for wet fluidized beds or the review by Caillet and Adelard[15] on sludges in anaerobic digestion.

This concise review article aims to give a general overview of this topic, addressing the main techniques that are used to perform CFD simulations of cohesive solids. To have a more generalized outlook, the content will also cover some materials that, despite comprising solid particles, are generally not labelled as 'granular', such as clays and sludges, which are very relevant in several engineering applications. This allows us to better describe the differences in the applied techniques depending on the scale of the system and of the involved particles.

The review starts with a description of the main types of cohesive forces that can be encountered in granular systems. The following section gives an overview of the relevant computational techniques, ascribing them to three main categories at a growing level of computational complexity. Each of these three categories is then treated separately: we start by addressing the main features, strengths, and weaknesses, and then we mention some recent research breakthroughs.

We wish to emphasize that our aim is not to cover the whole existing literature, nor to explore all the most recent advances in the simulation of these systems, which would be too extensive for such a wide topic and make compiling and reading this work unpractical. This work shall rather be considered as a starting point for readers who wish to get a general overview of this topic and identify more easily specialized publications. Although there are several published reviews and books that deal with specific aspects, a generalized and succinct outlook on this matter is difficult to identify.

2 | TYPES OF COHESIVE FORCES AND THEIR CHARACTERISTICS

Cohesive forces may arise from either particle intrinsic properties or external causes (most notably, but not exclusively, the presence of liquid water bridges between particles). In this section, a general classification of these forces is provided, describing their effects and intensity. Readers who are interested in more detailed descriptions of such forces may refer to the literature.[16,17]

A spontaneous cohesive behaviour and its intensity are so relevant to the overall behaviour of granular materials that it has been employed to classify particles. One of the best-known classifications dates back to 1973 and was proposed by Geldart[18] to discriminate particles according to their gas fluidization patterns. The validity

of this classification after 50 years has recently been confirmed and discussed by Cocco and Chew,[19] who provided the simplified depiction visible in Figure 1. For the purposes of this review, the fact that Group C is labelled as 'cohesive' immediately stands out, but some scholars have also ascribed the differences in the fluidization behaviours of Group A and B particles to the relative magnitude of cohesive forces. Severe operating conditions (such as high temperatures and pressures) may also accentuate the cohesive behaviour, with aeratable and sand-like particles possibly behaving as cohesive particles.[20] In general, the behaviour of cohesive particles is much more complex, and especially for Group C particles there are still several doubts on how to correctly describe their fluidization behaviour.[13]

From Figure 1, it is clear that particles with the most spontaneous cohesive behaviour are also the smallest. In other words, for these particles, the magnitude of cohesive forces exceeds that of the other forces (most notably gravity). This is caused by **van der Waals forces**, a class of different forces (caused by dipole/dipole, dipole/non-polar, or non-polar/non-polar interactions). They act between molecules and are always present to some extent. The force magnitude can be expressed for sphere-sphere interactions as follows:

$$F_{vw} = \frac{AR}{12a^2} \tag{1}$$

in which A is the Hamaker constant (whose magnitude depends on the involved materials), R is the sphere radius, and a is the surface separation. Although in the equation R should be the particle radius, this is only valid for ideally smooth spheres; as Seville et al.[16] showed, in practice this would result in an overestimation of the force. R has to be considered instead as the particle surface roughness, with the force magnitude thus becoming independent of the particle size (although, in practice, it has been observed that smaller particles and wide size distributions enhance cohesiveness[21]). When the previous equation is practically applied, the surface separation is also assumed to cap at a set minimum value (a_{min}) to avoid an infinite value for the force. The Hamaker constant can be also related to the material surface energy, for example employing the well-known Johnson–Kendall–Roberts (JKR) model.[22] According to this model, the force required to break an adhesive contact can be calculated as follows:

$$F_{off} = 3\pi E_s R^*_{ij} \tag{2}$$

in which R^*_{ij} is the reduced particle ratio (calculated as $(R_i \times R_j)/(R_i + R_j)$, with R_i and R_j being the radii of the two involved particles), and E_s is the surface energy. Equalling the two expressions, one can obtain the following:

$$E_s = \frac{A}{18\pi a^2_{min}} \tag{3}$$

In various works, the observed phenomena are discussed in terms of the surface energy rather than the Hamaker constant.

While van der Waals forces are always present, **electrostatic forces** arise because of how particles are handled. When a particle contacts with another one or with the wall it may exchange electrons, ultimately becoming electrically charged. The electrostatic force acting between two charged particles can be expressed through Coulomb's law, as follows:

$$F_e = \frac{1}{4\pi\varepsilon}\frac{Q_1 Q_2}{r^2} \tag{4}$$

in which ε is the permittivity of the medium, Q_1 and Q_2 are the charges of the two particles, and r is their separation distance. This force is usually negligible compared to van der Waals forces for fine particles and can be controlled by increasing the relative humidity in the surrounding gas.[23] Compared to the simpleness of the above equations, models that predict the process of particle charging are much more elaborated. The recent review by Zhao et al.[24] describes in much higher detail the features and behaviour of electrically charged particles.

Contrarily to the previous forces, particles may also tend to coalesce because of external agents. The most

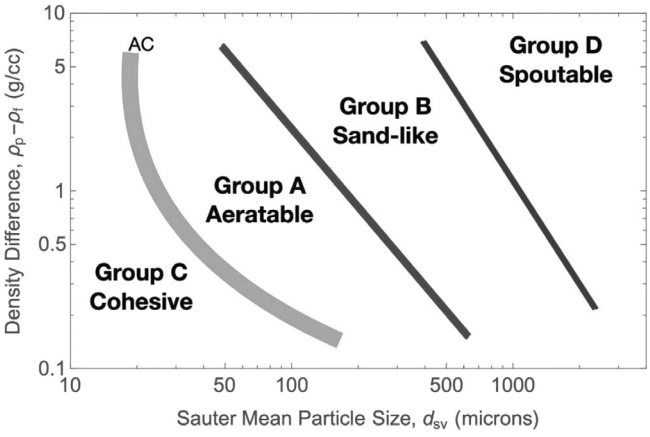

FIGURE 1 Interpretation of the Geldart classification (from Cocco and Chew,[19] available under a CC BY 4.0 licence; ρ_p and ρ_f are the densities of the particle and the fluid, respectively).

common and widely studied of such agents is liquid water (i.e., the case in which particles are wet). When some water is present among particles, a liquid bridge connecting two particles may form, as Figure 2 depicts. This creates a cohesive force (**liquid bridge force**) due to both the pressure drop in the liquid bulk and the surface tension of the fluid. Even for simple spheres, expressing the magnitude of the capillary force is a complex task; various degrees of accuracy can be attained and in recent years numerical simulations have also been employed for this purpose. The recent article by Yang et al.[25] and the review by Xu et al.[12] describe some of the existing models. Through some approximations, however, it is possible to obtain this simple expression for the maximum static capillary force for two identical spherical particles:

$$F_{\mathrm{cap,max}} = 2\pi R_{\mathrm{p}}\gamma, \tag{5}$$

in which R_{p} is the particle diameter and γ the surface tension of the liquid. In addition to the previous considerations, the equation's formulation may be complicated if the particle surface asperities are taken into account as well. For bridges formed by liquid water, the equation above yields forces that are always more intense than van der Waals forces.[16]

It also has to be noted that the intensity of the bridge force depends on the saturation degree, as Figure 3 shows schematically. For unsaturated cases, three regimes can be identified, depending on the shape of the liquid bridges and the amount of gas among particles: pendular, funicular, and capillary. The cohesion degree at first increases very sharply with the saturation degree in the pendular state, but remains mostly constant in the funicular state, and sharply decreases in the capillary state (readers who have tried building sandcastles may have some familiarity with these concepts). When particles are fully immersed in a liquid and form a slurry, bridge forces completely disappear. However, the particles may still behave as cohesive, for example if they experience significant van der Waals forces. The influence of liquid bridge forces and their consequences in practical applications have been the object of various experimental studies[26–28] and also of computational ones, as detailed in the following sections. Generally speaking, this aspect is both scientifically intriguing and relevant for practical applications; the presence of even small quantities of water may noteworthily affect the behaviour of particles, to the extent that separate classifications may be needed.[29]

Finally, particles may also cohere because of **other forces**, which are less addressed in the literature; these include the presence of organic matter, such as various types of organic residues, that may also act as a binder for particles, forming agglomerates and influencing the behaviour of the fluid–solid mixture. This is particularly relevant for materials where biological activities are abundant, such as sludges. Additionally, some kind of

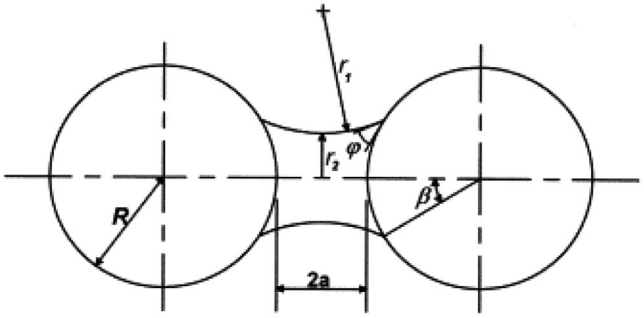

FIGURE 2 Depiction of a liquid bridge between two identical spheres; reprinted with permission from Seville et al.[16]

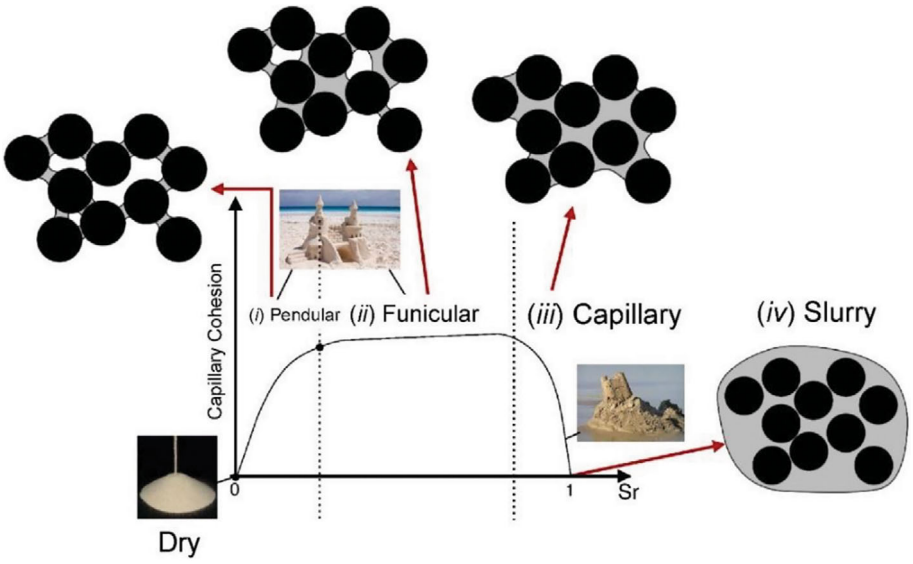

FIGURE 3 Schematic representation of different unsaturated systems, with Sr indicating the saturation degree. Adapted with permission from Tahmasebi.[4]

particles may soften or partially melt when subjected to severe temperature and pressure conditions, modifying their collision behaviour and possibly also creating cohesion phenomena.

3 | OVERVIEW OF CFD MODELLING APPROACHES FOR COHESIVE FLUID–SOLID SYSTEMS

CFD simulations can reproduce the behaviour of a unit or system based on the chosen set of equations, the specified control volume and initial and boundary conditions. While at the beginning CFD was mainly based on self-written codes and rudimental computers, its availability and popularity have skyrocketed and nowadays it is a staple tool in various sectors, thanks to the development of various commercial and open-source programs and the exponential growth in the computational capacity of modern computers. The core of CFD is the numerical solution of the local balance equations of mass, momentum, and energy (although the energy equation is often neglected, if the system is isothermal). For a multiphase system with no chemical reactions and phase transfers, they can be written for a generic fluid phase q as follows:

$$\frac{\partial}{\partial t}\left(a_q \rho_q\right) + \nabla \cdot \left(a_q \rho_q \vec{u}_q\right) = 0 \tag{6}$$

$$\frac{\partial}{\partial t}\left(a_q \rho_q \vec{u}_q\right) + \nabla \cdot \left(a_q \rho_q \vec{u}_q \vec{u}_q\right) = -a_q \nabla p + \nabla \cdot \vec{\vec{t}}_q + a_q \rho_q \vec{g} + \vec{R}_{pq} \tag{7}$$

$$\frac{\partial}{\partial t}\left(a_q \rho_q h_q\right) + \nabla \cdot \left(a_q \rho_q \vec{u}_q h_q\right) = a_q \frac{\partial p_q}{\partial t} + \vec{\vec{t}}_q : \nabla \vec{u}_q - \nabla \cdot \vec{q}_q, \tag{8}$$

In these, a_q is the volume fraction of phase q, ρ_q its density, $\vec{u}_q$ its velocity, p the pressure, and h_q the specific enthalpy. $\vec{R}_{pq}$ is the momentum exchange between the gas and solid phases (not treated here, but discussed in various works[9]). In the second equation, $\vec{\vec{t}}_q$ is the stress–strain tensor, expressed as follows:

$$\vec{\vec{t}}_q = a_q \mu_q \left(\nabla \vec{u}_q + \nabla \vec{u}_q^T\right) + a_q \left(\lambda_q - \frac{2}{3}\mu_q\right) \nabla \cdot \vec{u}_q \vec{\vec{I}}, \tag{9}$$

where μ_q and λ_q are the shear and bulk viscosity of phase q.

These equations are solved over the whole specified geometry, priorly discretized into a computational grid. Several additional closure equations are required to correctly account for the various involved phenomena (most notably turbulence, since the Navier–Stokes equations are usually solved in their Reynolds-averaged form[30]).

CFD was originally developed to study the behaviour of pure fluids (usually water or air) and is in many cases still applied to this purpose. Nonetheless, oftentimes natural and industrial cases of interest involve more than one phase, further complicating the modelling set-up. In principle, this would always be the case if one wants to study the interaction between solid particles and a fluid, which is also the object of this review. Researchers have proposed several approaches to account for multiphase systems. For the sake of conciseness, here we will categorize them into three main groups, loosely following the classification proposed by Pan et al.[31]:

- Pseudo-single phase approaches. In selected cases, a slurry consisting of a liquid and fine solid particles can be simplified as a unique continuous phase, with a reduction in the computational complexity. To account for the presence of the particles, a proper model for the slurry's viscosity needs to be included in the simulation. Oftentimes, the interparticle cohesion forces make the slurry behave as a non-Newtonian fluid, thus showcasing a non-constant viscosity. If a gas phase or another liquid is also included, the approach can be labelled as 'pseudo two fluid', and the two phases are often simulated through simplified methods, such as the volume-of-fluid (VOF).
- Eulerian–Eulerian approaches. They consider both the fluid and the solid phases as interpenetrating continua, which can coexist within the same cell with different velocities and properties. For this reason, such methodology is often labelled as 'two-fluid method' (TFM). Many closure equations are employed to correctly account for the behaviour of the solid phase, and further modifications are required to consider cohesiveness. Although this approach is often labelled as less accurate and informative, it represents a valid compromise due to its limited computational complexity, particularly when dealing with systems comprising high numbers of particles.
- Eulerian–Lagrangian approaches. They consider the fluid phase as a continuum, while the particles as discrete elements. The trajectory of each particle is tracked via the numerical solution of its equations of motion. The computational complexity of this approach scales with the total number of particles, becoming prohibitive for various realistic systems. However, it is also generally deemed as more accurate and can provide more detailed results. Particle–particle collision forces are directly modelled employing the

discrete element method (DEM): this coupling is hence known as 'CFD-DEM'. There are also other methods employing statistical approaches to account for inter-particle interactions but are thus far less established.

Although moderately simplifying the matter, it could be said that the suitability of one approach over the other mainly depends on the size of the simulated particles, moving from microscopic ones to rather coarse ones, or of the control volume. In the following sections, each of these methodologies will be described in better detail, describing the most salient recent research articles that employ them for the systems of our interest.

Again, we wish to emphasize that the current review only focuses on cohesiveness, but each of the aforementioned methodologies also has other open questions and a lack of agreement on various aspects. Most notably, both the TFM and the CFD-DEM require including a model to account for the fluid–solid drag force, which arises due to the slip velocity between the two phases. Although various models exist, there is no consensus on the most suitable one for the various applications, and additional problems in the formulation of the drag model arise when the particles are not monodisperse.[8,9]

4 | PSEUDO-SINGLE PHASE APPROACHES

When dealing with a slurry consisting of solid particles in a liquid, simulating it as a single pseudo-phase may represent a reasonable simplification. Clearly, this is only feasible if some requirements are met. Relevant cases may be liquid slurries with low concentrations of solid particles, or fluids in which fine particles are evenly dispersed and do not tend to separate spontaneously. Such an assumption reduces the number of equations to be solved, making the simulations significantly faster and thus making them suitable even for the large scales of industrial reactors or natural phenomena. Drawbacks are the lower accuracy and the loss of information on the solid phase, which becomes 'invisible' and uniform.

This approach can also be extended to cases in which, in addition to the slurry, another phase (such as a gas) is also relevant; if the slurry and the additional phase are immiscible, it is possible to employ a pseudo-two-phase approach, using interface methods such as the VOF, typically applied for liquid–gas (or–vapour) or oil–water systems. The VOF method was originally proposed by Hirt and Nichols in 1981.[32] Contrarily to Eulerian–Eulerian and Eulerian–Lagrangian approaches, treated in the following sections, this approach is based on the assumption that the two (or more) phases cannot coexist within the same computational cell. Therefore, only one set of balance equations is solved for all phases, and the interface between them is tracked through an additional transport equation for the phase volume fraction. The advantages of this approach lie in the lower number of equations to be solved, simplifying the set-up specification, reducing the number of required parameters and lowering the computational complexity. These benefits cannot be overlooked for applications at large scales.

To accurately describe the slurry's flow, it is vital to properly model its viscosity. The study of the flow behaviour of a material, with emphasis on the relationships between stresses and strains, is known as 'rheology', while the word 'rheometry' groups the experimental techniques that focus on this aspect.[33] For water and pure Newtonian fluids in general, the viscosity can be considered to only depend on temperature. Therefore, for a fixed temperature, there is a direct linear relationship between stress and strain. Many types of slurries encountered in nature and industrial applications instead display relationships that are not linear and are therefore labelled as non-Newtonian. Figure 4 shows the different behaviour of Newtonian and non-Newtonian fluids through generic stress–strain plots.

The presence of cohesive particles in a slurry does not necessarily imply that the slurry will show non-ideal rheology, provided that the particle concentration is low. The presence of cohesive forces interparticle forces is also not the only factor that can cause a slurry to behave as a non-Newtonian fluid. Nonetheless, various categories of

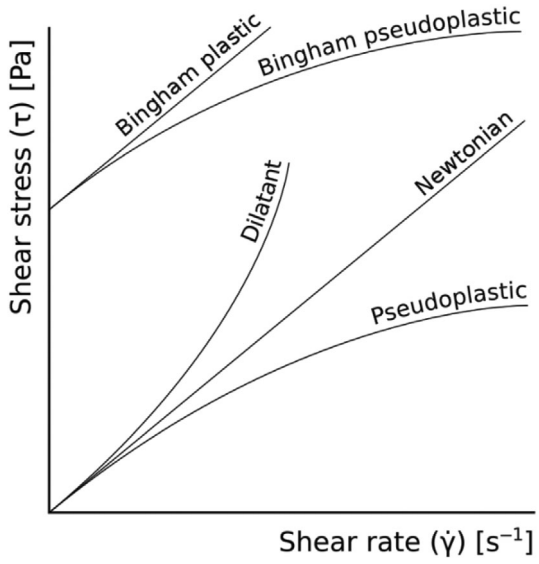

FIGURE 4 Behaviour of different types of fluids depending on their rheological properties (reproduced from commons.wikimedia.org/wiki/File:Rheology_of_time_independent_fluids.svg, available under a CC BY-SA 3.0 licence).

slurry materials display such behaviour by virtue of the presence of cohesive forces, noteworthy examples being sludges and clays. Various established models describe the viscosity of these materials with satisfying accuracy. The most common ones are the power-law, Bingham, and Hershel–Bulkley models, whose equations for the shear stress t_s are respectively as follows:

$$t_s = \eta \dot{\gamma}^n \tag{10}$$

$$t_s = t_0 + k\dot{\gamma} \tag{11}$$

$$t_s = t_0 + k\dot{\gamma}^n, \tag{12}$$

in which η is the non-Newtonian viscosity, $\dot{\gamma}$ is the shear rate, t_0 the yield stress, k the consistency index, and n the power-law index. It can be seen that the Hershel–Bulkley equation is the most general one: it can be reduced to the power-law equation if t_0 is 0, or to the Bingham equation if n is 1. The yield stress t_0 represents the minimum force that has to be applied for the fluid to start flowing. These models are available in the standard formulation of commercial CFD programs such as Ansys Fluent, so their implementation is often straightforward.

As already mentioned, sludges are one of the best examples of mixtures of liquid and microscopic particles that display a non-Newtonian behaviour. Given their ubiquity in any human settlement with wastewater treatment facilities and the necessity for their optimization, many researchers have devoted their efforts to the reproduction of the fluid dynamic behaviour of sludges. Most of such studies have dealt with the anaerobic digestion process, aimed at converting organic residues into a gaseous mixture of methane and carbon dioxide. Various review articles have summarized the breakthroughs and difficulties in performing CFD simulations of anaerobic digestors.[34,35] The recent review by Caillet et al.[36] provides a wide discussion of this topic, also categorizing the different aims and approaches that have been followed in the simulations. The same group had previously also published another review[15] that is more relevant to the scope of this work. In it, the authors summarize the rheological properties of wastewater, manure, and sludge, describing the main equations employed to describe the viscosity of non-Newtonian fluids and the required parameters. In general, the authors emphasize that, for a given material, the rheological behaviour depends on the solids concentration and temperature,[37] which can change during the process itself. Thus, in some cases, user-defined functions are employed to include the dependence of the parameters of Equations (10)–(12) on these variables, as they are not included in their standard formulations.

The non-Newtonian behaviour can usually be observed when the solids mass fraction exceeds 2%.[38] Its occurrence is also highly dependent on temperature: higher temperatures are known to decrease the viscosity and, in some cases, change sludges' behaviours to Newtonian. This effect is at least partly irreversible, depending on the intensity of hydrolysis reactions that are favoured by higher temperatures. However, the viscosity is often measured at ambient temperature or slightly above it. Accurate models accounting for the changes in the viscosity of a fluid as a function of time and temperature are mostly lacking. Rather than for anaerobic digestion, this is particularly a problem for more severe processes, such as thermal hydrolysis or hydrothermal carbonization (HTC).[39] These are often applied to facilitate the initial hydrolysis phase and enhance the biogas yield, employing treatment temperatures of 120–250°C in pressurized conditions. Some researchers[40–42] have measured the changes in viscosity that such treatments bring, but only after the obtained products had been brought back to ambient temperature. If one wanted to perform a CFD simulation of thermal hydrolysis or HTC, they would be hindered by the lack of rheological data for the actual process conditions. This was the case in the recent work by Marchelli and Fiori,[43] who proposed a preliminary approach based on a user-defined modification of Ansys Fluent to consider the decrease in sludge viscosity when simulating the heating phase of an unstirred HTC reactor. A common observation in CFD studies is that the non-Newtonian rheology hinders the mixing within the digestor and creates asymmetrical profiles, as Figure 5 shows as per the work of Craig et al.[44] In the framework of modelling bioreactors, the recent work by Sadino-Riquelme et al.[45] discusses the difference between considering single-phase or multiphase approaches while also considering non-Newtonian rheology and mechanical mixing.

Moving to another field of application, various types of materials found in the environment have been described through similar approaches, such as soil, clay, and sand. Despite the wide temporal and spatial scales that the phenomena affecting these materials may involve, some of their properties and behaviours are comparable to fluidized beds or other units typical of process engineering.[46,47] Various studies have investigated the rheological properties of materials such as muds,[48,49] natural sediments,[50] flotation slurries,[51] clays,[52] and so forth. The models that are suitable for describing the viscosity of these materials are often the aforementioned ones (Hershel–Bulkley, Bingham, or power-law models). CFD studies on their behaviour are scarce, and more often they have been analyzed through analytical methods.[53] Nonetheless, some studies exist. A 2014 study by Chen et al.[54] coupled the VOF with the finite

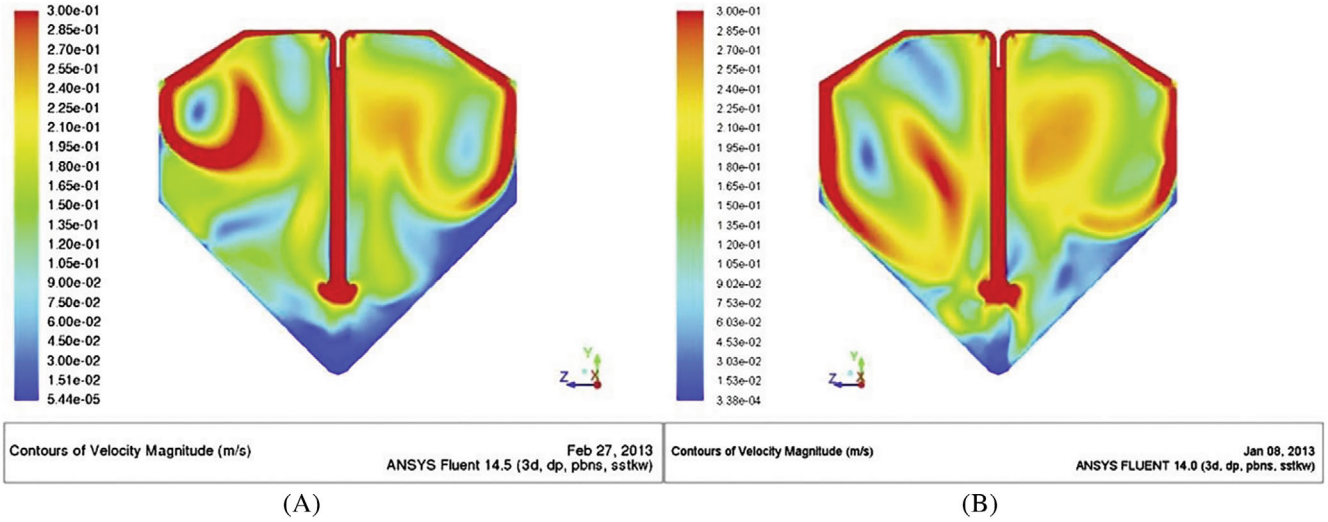

FIGURE 5 Flow patterns of (A) raw sludge and (B) digested sludge in an anerobic digester. Adapted with permission from Craig et al.[44]

element method (FEM) to simulate the process of fracture grouting in soils. VOF is employed to simulate grout and water as two separate phases, and the authors employ an empirical equation to express the viscosity of grout, taking into account its variation with time. The same case study and approach can be encountered in the work by Zhang et al.,[55] who discussed in higher detail how to consider the variation of the viscosity in the modelling. VOF was also chosen by Wang and Song[56] to reproduce deepwater jet excavation: their simulation considered water and cohesive soil, with the latter's rheology being described through the Herschel–Bulkley model. Wang et al.[57] studied a similar problem but focused on the jet deflection employing the mixture approach for the simulations and the Bingham model for the rheology of the soil. The Bingham model was also employed by Lovato et al.[58] to simulate the motion of a plate through mud. A different approach was followed by Gharib et al.[59]: these authors first performed CFD simulations of paste backfill flowing into a tube and then employed the obtained fluid dynamic profiles in DEM simulations to obtain information on the wear of the apparatus.

Other researchers followed analogous approaches to simulate various types of slurries, such as a suspension of kaolin in water,[60] coal ash slurries,[61] bentonite slurries,[62] metal mines slurries,[63] slurries from lignocellulosic biomass hydrolysis,[64] generic slurries in which macroscopic particles settle,[65] and so forth.

In summary, pseudo-single phase approaches represent valid tools that, when applicable, can be employed as practical compromises even for large-scale applications. The CFD algorithm and the models for non-ideal viscosity are mostly established, so the problems in practical cases are mostly ascribable to other aspects, that require instead more advanced experimental investigations. Perhaps the most notable is a proper description of the viscosity of materials (most notably sludges) as a function of the solids concentration and applied temperature, possibly considering also the relevant chemical and biological reactions. Including reactions can be problematic for various processes as well, due to the very different involved time scales, but there are stratagems to employ.[34]

5 | EULERIAN–EULERIAN METHODS

In Eulerian–Eulerian (E–E) simulations, both fluid and solid phases are treated as interpenetrating continua. For this reason, this approach is also known as the two-fluid-model (TFM) or multi-fluid-model (MFM), depending on the number of involved phases. The phases can coexist within the same computational cell with a certain volume fraction; the algorithm solves a separate set of the mass, momentum, and energy balance equations for each involved phase. The solids momentum equation is analogous to Equation (7), with an additional term on the right-hand side ($-\nabla p_s$) accounting for the solids pressure. As a matter of fact, to reproduce the behaviour of the solid phase despite the continuum hypothesis, an extensive set of closure equations needs to be included. These equations rely on the kinetic theory of granular flows (KTGF), which is based on the kinetic theory of gases and introduces some related quantities, such as the already mentioned solids pressure. The pivotal variable is the granular temperature (Θ_s), which is a measure of the

particle kinetic energy and is in principle equivalent to $u_s^2/3$. In practice, in simulations Θ_s is calculated by solving either another transport equation or an algebraic equation. In both cases, other sub-models and parameters are needed, one of them being the restitution coefficient (e_{ss}), a measure of the fraction of energy that is retained by particles after colliding (being 1 for completely elastic collisions and 0 for completely inelastic collisions).

In the context of cohesive particles, a very relevant variable is the viscosity of the solids, which in the KTGF depends on three contributions: the frictional viscosity ($\mu_{s,fr}$), the collisional viscosity ($\mu_{s,col}$), and the kinetic viscosity ($\mu_{s,kin}$). These are summed to obtain the total solid viscosity as follows:

$$\mu_s = \mu_{s,fr} + \mu_{s,col} + \mu_{s,kin} \tag{13}$$

These terms are usually calculated employing models proposed by Schaeffer et al.,[66] Gidaspow et al.,[67] and Syamlal et al.[68] The KTGF also calculates the solids bulk viscosity (λ_s), which accounts for the resistance of granular phases to compression and expansion and is usually given as follows[69]:

$$\lambda_s = \frac{4}{3}\alpha_s \rho_s d_s g_0 (1+e_{ss}) \left(\frac{\Theta_s}{\pi}\right)^2, \tag{14}$$

where g_0 is the radial distribution function. Readers who are interested in a more detailed resume of the KTGF and its equation may refer to the numerous related works published in the literature, such as the one by Wang.[70] The work by Macaulay and Rognon also provides some interesting considerations on the concept of viscosity for cohesive solids.[71]

The TFM has some peculiar advantages: the computational demand is generally not excessive and does not depend on the total number of involved particles, thus being also suitable for large-scale applications or systems involving micrometric particles. Moreover, there are no constraints based on the size of the particles and of the computational mesh, which is instead the case for the Eulerian–Lagrangian methodology (as addressed in the next section). However, the method has often been deemed as less accurate, and the results that it provides are not as detailed. Moreover, it is unable to yield particle trajectories, which may represent useful information in various cases.

The TFM has been chosen for various applications, such as traditional fluidized beds,[72] circulating fluidized beds,[73] spouted beds,[74] cyclones,[75] feeders,[76] particle transport,[77] study of soil and sediments,[78,79] proppant transport in hydraulic fractures,[80] and so forth. Moreover, it has been applied to various types of particles, from very fine to rather coarse, thanks to its ability to function mostly regardless of the particle size. The method has also been employed to simulate non-spherical biomass particles, in some cases through ad hoc modifications of the equations of the KTGF.[81]

Albeit useful and practical, the KTGF was developed considering perfectly elastic spherical cohesionless particles in dry conditions. Therefore, if one wants to include interparticle cohesiveness in TFM simulations, either the KTGF equations must be modified, or additional modelling tools must be included. The following sections will discuss the approaches followed by different researchers to include cohesiveness in CFD simulations. A few authors have also discarded completely the KTGF and performed Eulerian–Eulerian simulations with models for the solids viscosity comparable to those of the previous section,[82] which is indeed adequate even when considering fluidized bed emulsions of cohesionless particles.[83,84]

5.1 | E–E simulation involving van der Waals forces

Adapting the KTGF for cohesive solids has puzzled many researchers over the years and Geldart-A particles in fluidized beds have been a noteworthy case study. Perhaps the first example of such modifications was proposed in 2002 by Kim and Arastoopour,[85] who employed a mathematical approach to take into account the contact bonding energy loss due to particle agglomeration in an updated version of the KTGF. The model was later modified by Huilin et al.,[86] who introduced the concept of agglomerate diameter. The agglomerate diameter approach had also been attempted by van Wachem and Sasic[87] as the variable to be calculated from a force balance, but without modifying the other equations of the KTGF. This way, a local particle size distribution is obtained, with each size class being modelled as a different solid phase. Another modification was proposed by Ye et al.[88] through a correction factor called 'excess compressibility' to account for interparticle cohesion. The two aforementioned methods, both valid for mildly cohesive Geldart-A particles, were compared by Wei et al.[89] Pointing out the lack of criteria for the determination of the employed parameters, the authors proposed some possible procedures. Then, they showed that the two methods have different advantages, and none is strictly superior to the other, but both represent improvements compared to the standard KTGF.

In other works, the KTGF was not modified and drag corrections were instead put in place. This is because

cohesive forces lead to the formation of agglomerates, and the fluid–solid drag force is affected by their presence. For example, Ahmadi Motlagh et al.[90] considered the case of dry Geldart-A particles. They discussed in detail the particle and agglomerate force balance, ultimately coming up with a correction term for the Wen–Yu drag equation. An entirely new drag model was proposed by Luo et al.,[91] who managed to simulate a gas–solid fluidized bed and obtain much better results than those produced by the Gidaspow and Syamlal–O'Brien drag models.

Another possibility is coupling the TFM with a population balance model (PBM), which can describe the aggregation frequency and coalescence efficiency. The review by Jeldres et al.[92] describes this approach in much higher detail. The PBM introduce a new differential equation, called the population balance equation (PBE),[93] which describes the transport of a function representing the number density of particle agglomerates with a certain diameter. It has this form:

$$\frac{\partial}{\partial t}(n(L)) + \nabla \cdot \left(\vec{u}_s \cdot n(L)\right) = -\frac{\partial}{\partial t}(G(L)n(L)) + B_{\text{nuc}}(L) + Q_{\text{agg}}(L) + Q_{\text{frag}}(L), \tag{15}$$

in which $n(L)$ is the number density of particles with diameter L, G the particle birth rate due to chemical reactions, B_{nuc} the rate of nucleation, and Q_{agg} and Q_{frag} the net rates of aggregation and fragmentations.

The solution of this equation requires a specific method, with the most common ones being the Monte Carlo, discrete methods, and methods of moment (MOM).[94] The first one is hard to integrate into common CFD programs and is thus uncommon.[95] The discrete methods approach relies on discretizing the agglomerate size distribution in a finite number of classes.[96] The advantage is that the agglomerate size distribution is directly calculated, but the classes have to be defined at the beginning, have to be simulated as separate phases, and may be numerous. Conversely, the MOM[97] considers only the moments of the PBE, thus only requiring a few scalar equations to be solved throughout the simulation. More detailed information on the particle size distribution is lost, and case-specific parameters are still needed. Updated versions of the MOM, such as the quadrature MOM (QMOM)[98] or the direct quadrature (DQMOM)[99] have been proposed in recent years and have become rather popular in this field. This methodology has been employed by various authors in recent years; Thakur et al.[100] summarized some of them for the case of polyolefin slurry reactors. Other authors have proved this method as suitable for spouted beds[101] and circulating fluidized beds.[102]

All the previous approaches have strong points and shortcomings, and no choice has still emerged as superior nor is considered established. Some authors also operated by enhancing them in a combined fashion, such as the groups of Zheng[103] and Kellogg.[104] The latter coupled PBM with the KTGF, considering the granular temperature to modify both of them. In particular, for the PBM they considered that the agglomeration/breakage probability is not constant but is a function of Θ_s, and in the KTGF they included a variable restitution coefficient. Both in the aforementioned work and in a following one,[105] the authors showed that the values of the employed parameters can be obtained through DEM simulations, which allow measuring interparticle force magnitudes for particles with diameters lower than 100 μm. The simulation approach was successfully tested for a fluidized bed riser.[106]

In another recent breakthrough, Askarishahi et al.[107] argued that the aforementioned updates of the KTGF may find success for selected applications but are ultimately relying on unsound bases since the KTGF was not envisioned for cohesive particles. There is hence the need for a robust rheological model to properly introduce the cohesive force. They employed the recent one by Gu et al.[108] and introduced it in the code of the open-source program MFiX, modifying the equations of the granular energy and solids viscosity and pressure. They tested various degrees of cohesion (as shown in Figure 6) and obtained a regime map for fluidized beds.

In summary, the Eulerian–Eulerian simulation of such systems is far from established, and there are still ample margins for improvement. The common programs that are used for these simulations often do not include most of the suitable equations, thus their codes have to be modified ad hoc, which may be particularly time and resource-consuming. For specific cases, however, simplified approaches may be acceptable and not entail excessive complexity for the simulation set-up.

5.2 | E–E simulations involving liquid bridging

The length of the previous sub-section proves that TFM modelling of inherently cohesive particles has received attention in recent years, even though no established methodology has yet emerged. For the case of wet particles, instead, the amount of published literature is much scarcer. This gap may be attributed to the higher complexity of the liquid bridge force compared to the van der Waals force. Its magnitude is indeed not a constant particle property but is affected by the characteristics and amount of the liquid that surrounds the particles.

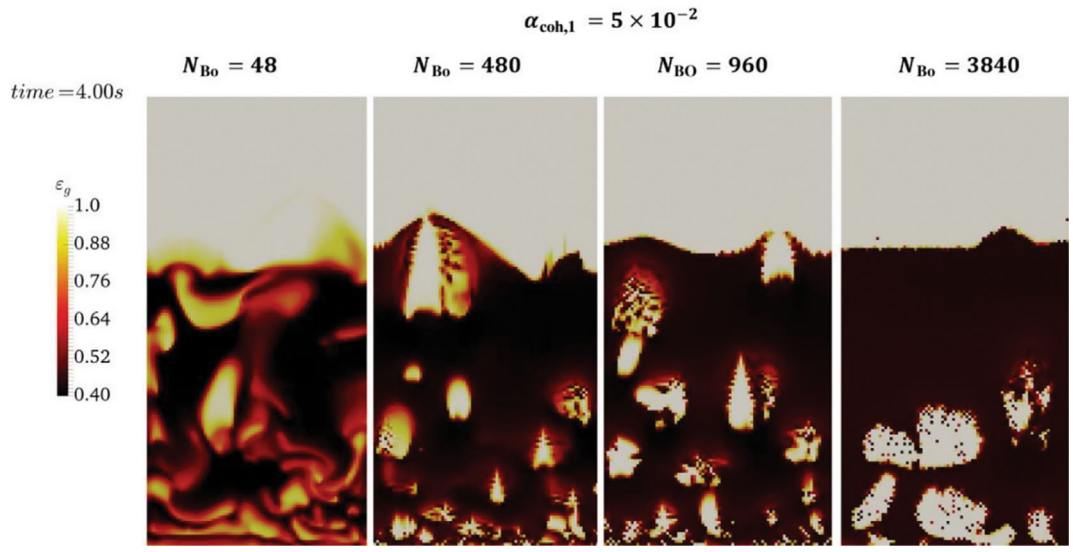

FIGURE 6 Effect of the Bond number on the instantaneous voidage distribution in a fluidized bed; reproduced from the work of Askarishahi et al.,[107] available under a CC-BY 4.0 licence.

It may therefore be easier to directly model the force as Eulerian–Lagrangian approaches allow, rather than indirectly including its effect in the KTGF. Nonetheless, few works have dealt with this task through the TFM, following two different approaches: the inclusion of PBM or the use of a non-constant restitution coefficient.

For the case of PBM, a pioneer attempt was published by Rajniak et al.[94] in 2009, focusing on the case of a Wurster-type granulator. In this case, the population balance was solved through the QMOM as well. The authors commented on the good performance of the simulations compared to experimental data but noted that the procedure was quite computationally expensive, limiting its applicability and the possibility of tuning parameters. Another more recent effort came from Ahmadi Motlagh and colleagues,[109] who considered a fluidized bed with injections of different liquids. Significant advances in their work were the modelling of the liquid phase, also involving its vaporization and abrasion and fragmentation of the particle clusters. Among the difficulties in developing these kinds of models, the authors pointed out that suitable experimental data are difficult to obtain.

Both previous studies focused on granulators, in which the formation of clusters is desired and frequent. Zhong et al.[110] argued that for a standard wet fluidized bed, coalescence is weaker and the PBM-based model introduces excessive complexity and uncertainty. Therefore, they proposed instead to modify the particle-particle restitution coefficient, employing the model proposed by Davis et al.[111] In the model, implemented in Ansys Fluent through user-defined functions, the restitution coefficient is a function of the liquid viscosity, liquid layer thickness, and impacting velocity. The procedure was able to reproduce some of the features of wet spouted beds, but the authors noted that further modelling features and validations are required to enhance it. The same group later updated the modelling set-up[112] by considering the particle diameter non-constant, so as to reflect the effect of cluster formations. More details on the CFD simulation of the wet fluidization process are summarized in the recent review article by Xu et al.[12]

5.3 | E–E simulations involving electrically charged particles

Finally, a few authors also modelled systems comprising charged particles. Similarly to the previous cases, also for this phenomenon some authors[113,114] have simplified the matter and considered the cohesive force as constant and the particles as monodisperse, while others[115] have employed a PBM.[115] Interested readers may find more details on the simulation of such systems in the recent reviews by Chowdhury et al.[116] and by Grosshans and Jantač.[117]

5.4 | Final comments

To sum up this section, the Eulerian–Eulerian approach represents a valid tool for the CFD simulation of cohesive solid–fluid systems, despite its known shortcomings. Most of the published works have focused on systems affected by van der Waals forces, arguably because the other approaches cannot practically simulate realistic systems of this sort. Nonetheless, researchers have not

reached a consensus on the most suitable methodology to include cohesiveness in such simulations, and even in very recent times we have witnessed new methodologies being proposed or updated. As a consequence, commercial and open-source programs still do not include most of the tools that would be necessary to perform such simulations; oftentimes, the only solution is to modify these programs ad hoc, where applicable. These considerations hold even more valid for wet systems, which have been the focus of fewer investigations. The general establishment of Eulerian–Eulerian methodologies, including how to better deal with polydispersity[118] and other non-idealities, will undoubtedly facilitate further efforts in this direction, together with the development of more advanced experimental techniques.

6 | EULERIAN–LAGRANGIAN METHODS

Eulerian–Lagrangian approaches employ two opposite methods for the fluid and solid phases. The fluid phase is treated as a continuum, in the same way as in the TFM, while the solids are considered in their discrete nature. Each particle is individually tracked by solving its Newtonian equations of motion, which can be written as follows:

$$m_p \frac{d\vec{u}_p}{dt} = m_p \vec{g} \frac{\rho_p - \rho}{\rho_p} + \vec{F}_{fs} + \vec{F}_c \tag{16}$$

$$I_p \frac{d\vec{\omega}_p}{dt} = \frac{\rho}{2}\left(\frac{m_p}{2}\right)^5 C_\omega \left|\vec{\Omega}\right| \cdot \vec{\Omega}, \tag{17}$$

where m_p is the mass of a particle, $\vec{u}_p$ and $\vec{\omega}_p$ its translational and rotational velocities, $\vec{F}_{fs}$ is the net fluid solid force (which includes the drag, virtual mass, pressure gradient, and Magnus lift forces), $\vec{F}_c$ is the net contact force, I_p is the moment of inertia, and $\vec{\Omega}$ is the relative particle–fluid angular velocity. The term $\vec{F}_c$ includes all types of forces that a particle experiences due to the presence of another particle (or of a wall). Usually, it includes a collision and a friction term, but it can be adapted to also include various types of cohesive forces.

The collision forces between particles are most commonly calculated through a deterministic approach known as the discrete element method (DEM),[119] originally proposed by Cundall and Strack.[120] Its coupling with CFD is hence referred to as 'CFD-DEM'. This section focuses on the so-called 'unresolved CFD-DEM',[121] in which computational cells are larger than the simulated particles (usually at least 4 times larger[122]) and the fluid flow around each particle is not fully resolved. Other methodologies, based for example on Lattice-Boltzmann or immersed boundary methods, are able to describe the flow around each particle, but due to their extreme computational demands, they are not employed for full-scale simulations, but rather to obtain closure equations to employ at a larger scale.[123]

Another sub-classification is between the hard-sphere and the soft-sphere DEM. In the hard sphere approach particles do not overlap and collisions are instantaneous. This approach is less often employed because it requires smaller time steps, and is mostly convenient for dilute systems.[124] Conversely, in the soft-sphere approach, the small deformations that particles physically endure when contacting are considered by making them slightly overlap, and the magnitude of the cohesion force is calculated as a function of the overlap, as shown schematically in Figure 7. The collision force usually comprises two terms: one for the elastic contribution, and one for the kinetic energy dissipation. For this reason, the approach is also known as 'spring-dashpot'. The two terms can be calculated following a 'linear' or 'Hertzian' approach. The linear model requires the specification of a spring constant and a restitution coefficient and is simpler and more efficient, although inadequate in some cases.[125] The Hertzian model requires instead the specification of the material Young modulus and Poisson's ratio and employs more elaborate equations, thus resulting generally slower. Finally, the frictional term is usually calculated employing Coulomb's friction model.

CFD-DEM is generally considered to be more reliable than the TFM[126,127] and the results that it produces are more detailed. It can yield information such as the trajectories of single particles, the forces that act on them, their coordination number, and residence time distribution. However, the overall equations to be solved are much more numerous and this hinders its application for large-scale systems: the maximum number of particles that can realistically be taken into account ranges from a few hundred thousand to a few million, depending on the specifics of the employed computer and the duration of the simulation.

The slowness of CFD-DEM has led researchers to develop alternative methodologies to perform unresolved Eulerian–Lagrangian simulations. These usually follow two routes: lumping several real particles in larger computational particles or calculating the collision forces through statistical approaches. The use of larger computational particles (referred to as 'parcels') is known as 'coarse-graining' and has been successfully employed for a variety of applications.[128] In order to achieve a

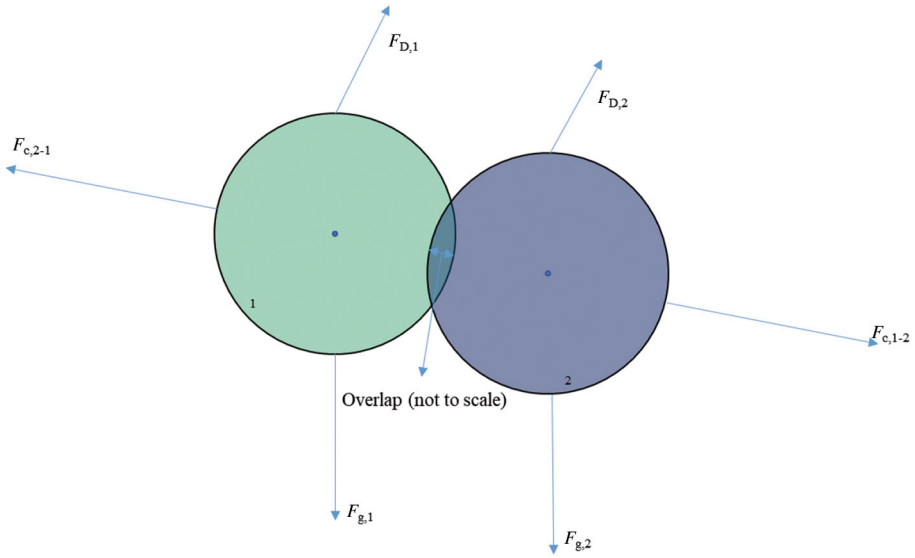

FIGURE 7 Schematic representation of two particles colliding in the soft-sphere approach; F_c, F_g, and F_D represent the contact, gravity, and drag forces, respectively.

similarity with the real system, some particle variables have to be scaled according to empirical correlations. Another problem of coarse-graining may lie in the need for using larger computational cells, which may hinder the prediction of the fluid flow. Coarse-graining simulations have been sporadically applied for cohesive systems.[129,130] The calculation of contact forces through statistical approaches is the core of some methods, such as the dense discrete phase method (DDPM,[131] available in Ansys Fluent) or the multiphase-particle in cell (MP-PIC,[6] available in Barracuda and MFiX). These approaches are based on the KTGF, and therefore would share the same problems of the Eulerian–Eulerian methods in including cohesiveness. However, as far as we are aware, the literature features no studies of this sort.

The CFD-DEM has been exploited for various applications,[132] including traditional and circulating fluidized beds,[133] spouted beds,[134,135] cyclones,[136] pyrolyzers,[137] blast furnaces,[138] inhalers,[139] soil erosion,[140] dust suspension,[141] snow,[142] erosion,[143] landslides,[144] medical studies,[145–147] and so forth. Due to the aforementioned limitations, it is mostly adequate for rather coarse particles, such as those belonging to the D group in Geldart's classification, but it also has been employed for smaller ones. It is also possible to reproduce non-spherical particles,[7] although the approaches to achieve this are still far from established, especially for non-ideal shapes.

Interparticle forces are directly calculated in CFD-DEM; specifying cohesive forces is hence more straightforward than in the TFM, and a larger number of related studies have been published. The review by Coetzee and colleagues provides a general overview of the models for cohesive forces employed in DEM simulations and the methods for calibrating parameters.[148] As mentioned in the previous section, some CFD-DEM studies have served the purpose of yielding parameters or relationships to be employed in other types of simulations. However, the approach has also been utilized to study more fundamental aspects of the behaviour of cohesive particles, such as the mechanisms of agglomeration.

6.1 | CFD-DEM simulations including van der Waals forces

Van der Waals forces can be directly included in each particle's Newtonian equation of motion. Since these forces are relevant for particles often quite small in size (with diameters of 100 μm or less), CFD-DEM may be too computationally demanding to achieve the desired results, for two reasons:

1. The number of equations to be solved depends on the number of particles, and realistic systems may involve millions or billions of micrometric particles, making their simulation prohibitive.
2. Even for lab-scale systems, the simulation duration is dictated by the time step of the DEM algorithm (Δt_{DEM}), which must be small enough to capture particle–particle collisions. Criteria such as the following one are usually suggested:

$$\Delta t_{\mathrm{DEM}} \leq \frac{1}{10} 2\pi \sqrt{\frac{m}{K}}, \tag{18}$$

in which m is the mass of the lightest considered particle, whereas K is the spring constant.

In some early works,[149–152] the cohesion force was not modelled according to a physically-based equation but simply considered to be a multiple of the particle weight, in order to study the fluidization of these particles from a fundamental point of view.

In the work by Ye et al.,[153] the van der Waals force is directly modelled following the Hamaker scheme, which requires as input the Hamaker constant and the minimum interparticle distance. Although the simulations allowed drawing some interesting observations on the fluidization of Geldart A particles in a 2D bed, the authors remarked that the study was still to be considered qualitative. In another work on fluidization, Moreno-Atanasio et al.[154] argued that the value of the spring constant K gains a greater influence on the observed fluidization patterns if the van der Waals force is also taken into account. In particular, if particles have high surface energy and the spring constant is set to a low value, fluidization is not initiated, and particles move as a block. The possibility to include van der Waals forces is by default available in the open-source program MFiX. This program has for example been employed by Galvin and Benyahia[155] to study the combined effect of cohesion, friction and particle polydispersity on the fluidization of Geldart A particles, while Li et al.[156] considered two different particle types and proposed a very thorough comparison with experimental observations, and finally Liu et al.[157] focused on the defluidization of fine particles, observing that the results are sensitive to the Young modulus (a major parameter in the non-linear Hertzian contact model). Fluidization of fine cohesive particles was also studied through CFD-DEM by the group of Yu: Hou et al.[158] studied various interesting aspects of the micromechanics of the fluidization of different powders, while Wu et al.[159] showed an approach to use the results of CFD-DEM simulations to model properties for Eulerian–Eulerian simulations. Fine cohesive particles were also simulated in spouted beds,[160] with the recent work by Zou et al.[161] offering interesting insights on the formation of clusters.

Considering the case of cyclones and a hard-sphere DEM, Almohammed and Breuer[162] studied the formation of particle clusters in more turbulent flows through two different agglomeration models, one based on energy and one based on momentum, deeming the latter as superior. Cyclones were also considered by Sgrott and Sommerfeld,[163] using a stochastic agglomeration model, and comparing two different approaches to assess the effect of the formation of agglomerates on the overall fluid dynamics. Some analogies may also be drawn with powder inhalers: their simulation approaches were reviewed by Sommerfeld et al.[164]

6.2 | CFD-DEM simulations of wet particles

To account for the cohesive force due to a liquid layer on the particle surface, two approaches are employed: one is based on directly adding the force to the particle's momentum balance, while the other accounts for the cohesion effect by modifying the particle–particle restitution coefficient. In both cases, more details on the CFD simulation of the wet fluidization process are summarized in the recent review article by Xu et al.,[12] while Song et al.[165] reviewed CFD-DEM studies of granulation and coating in fluidized beds.

Adding a further contact force between two contacting particles in the DEM algorithm is rather straightforward conceptually; nonetheless, a suitable model to calculate the force must be selected. Simplified approaches have been deemed adequate in certain conditions. For example, Xu et al.[166] simulated a flat-bottomed spouted bed through the CFD-DEM method by considering the cohesive force simply as a multiple of the particle weight, acting only when two particles are in contact. In particular, considering the surface tension and viscosity of water, obtaining the maximum particle velocity from the drag force and using the separation distance as a fitting parameter, the authors calculated that the cohesive force is about 10 times the particle weight. This value guaranteed a good resemblance with experimental data.

When the cohesive force is instead modelled following a physically based approach, researchers employ so-called 'liquid bridge force models'. The recent review by Xu et al.[12] classifies three of such models as the main ones employed in simulations, respectively originally proposed by Mikami et al.,[167] Liu et al.,[168] and He et al.[169] While the first one only considers a force contribution based on the capillary force (and hence on the liquid surface tension), the other two consider two contributions: a cohesive component due to the liquid's surface tension and a viscous component due to the liquid's viscosity. Figure 8 provides a depiction of the spouting behaviour of dry (above) and wet (below) particles employing the Mikami model, as per the work of Zhu et al.[170] For a more detailed resume of articles dealing with CFD-DEM simulations of wet fluidization through these approaches, readers are referred to the already cited review.[12] All three aforementioned approaches rely on further submodels to predict relevant inputs, such as the liquid bridge volume. In this framework, Wu et al.[171] commented that previous studies simplified this aspect by considering a static bridge model. The authors show that a more advanced model can indeed produce better results, but only in certain operating conditions, and propose heuristics based on dimensionless numbers.

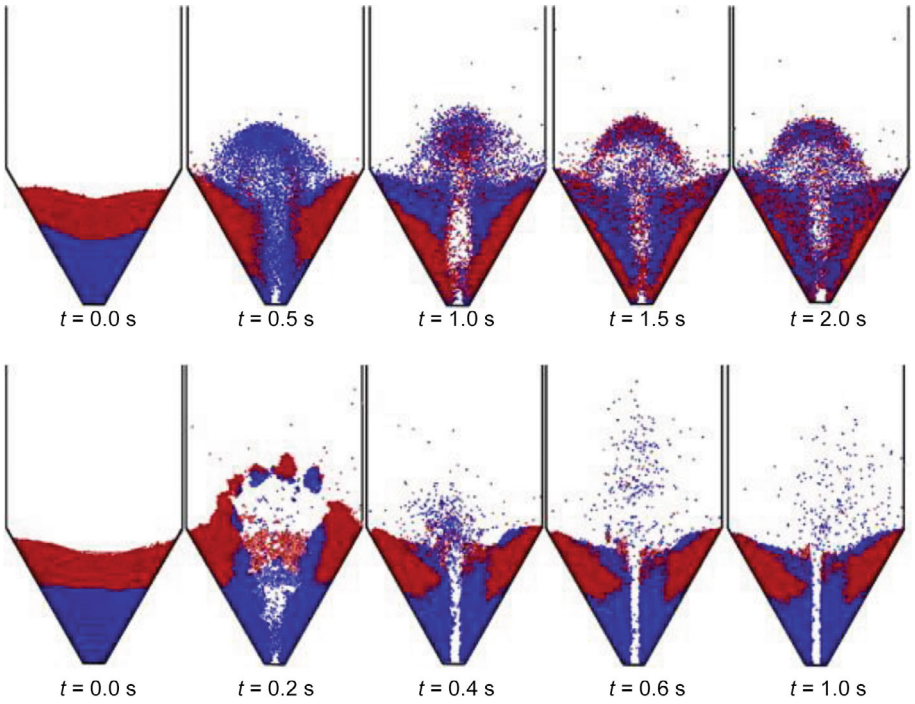

FIGURE 8 Spouting behaviour of dry (above) and wet (below) particles; adapted with permission from the work of Zhu et al.[170] The red and blue colours have no physical significance and merely serve to facilitate visualizing the mixing efficiency.

In a slightly different framework, Lu et al.[172] studied the sedimentation of polyethylene particles in liquid dodecane. These particles experience cohesive forces at high temperatures due to their swelling, leading to the formation of solid and liquid bridges. The cohesiveness is accounted for through a simplified version of the JKR model.[22] Along the same vein, particles may also stick and coalesce because of severe operating conditions that cause them to partially melt. This effect was first preliminarily addressed by Wang and Rhodes[173] considering the cohesion force as a multiple of the particle weight. Mansourpour et al.[174] calculated such force through a more detailed approach and simulated the formed agglomerates through the multi-sphere method, which in the literature has also been employed to mimic non-spherical particles. The recent work by Deng et al.[175] considered the case of particle spray coating, also taking into account the increase of the particle diameter as droplets collide with the solids. Following a more practical approach, Zhou et al.[176] employed CFD-DEM simulations to assess the effects of liquid content and surface tension on the fluidization characteristics, identifying conditions that enhance the overall phenomenon. Finally, Chan and Washino[177] addressed the scaling of the wet cohesive force when performing coarse-grained simulations, while Tausendschön et al.[130] focused on the same problem also taking into account van der Waals forces.

Conversely, in the second approach, both the cohesive and the viscous components are reproduced through the restitution coefficient, which is not considered as constant as for non-cohesive particles. This approach is generally simpler and accurate enough, but not directly modelling the surface tension can lead to an underprediction of the size and duration of clusters. One of the first examples is the work by van Buijtenen et al.,[178] who considered granulation in a spout-fluidized bed. One of the peculiarities of this work is also simulating the trajectories of water droplets and their collision with solid particles, which is usually neglected. The impact of the bridge force is accounted for by varying the restitution coefficient, which depends on the particle moisture content. A more thorough approach was later proposed by Darabi et al.,[179] employing a model they had previously developed.[180] Song et al.[181] also considered a variable restitution coefficient, emphasizing that the particle contact displays a hysteretic behaviour. Another model for the wet restitution coefficient was proposed by Davis et al.[111] and later updated by Sutkar et al.,[182] who also considered it in combination with the study of water droplet trajectories.[183] Variable restitution coefficients were also applied for other applications, such as the work by Saparbayeva et al.[184,185] considering a slurry of ice particles in oil.

6.3 | CFD-DEM simulations of electrically charged particles

Finally, some researchers focused on the case of electrically charged particles. One of the first efforts was published by Watano et al.[186] in 2003, using a simplified

model based on the collision velocity, to study powder pneumatic conveying. A more advanced model, based on the concept of successive condensers, was implemented by Pei et al.[187] to study fluidization and was subsequently applied in other works. Electrostatic forces and charging modelling were applied by Korevaar et al.[188] to study pneumatical conveying, showing that the effect is significant only above a certain value of the particle charge and that the results are sensitive to the particle charging efficiency. Other studies have focused on fluidized beds[189–192] and pharmaceutical devices.[193] Interested readers may find more details on the simulation of such systems in the recent reviews by Chowdhury et al.[116] and by Grosshans and Jantač.[117]

6.4 | Final comments

To sum up this section, Eulerian–Lagrangian simulations (virtually always based on the CFD-DEM approach) represent the most straightforward choice to study the effect of cohesive forces in particle–fluid systems. They have been successfully applied for both obtaining correlations to be employed in Eulerian–Eulerian simulations and to study fundamentals and practical aspects of cohesive systems.

With regard to van der Waals forces, there appears to be more consensus on the choice of the sub-model, as testified by its inclusion in established programs (such as MFiX). However, these simulations suffer from the high computational complexity entailed by micrometric particles. Coarse-grained simulations may overcome this issue, but currently they still represent a niche for such particles.

With regard to liquid bridge forces, various breakthroughs have been achieved, but the underlying problem is that the sub-models can be quite complex. New or updated versions of such models have been proposed even recently, also thanks to the growth of advanced simulation and experimental techniques. As such, simulating wet systems still relies on the user doing ad hoc modifications of the employed code. Moreover, most of the studies have focused on spherical particles. This allowed notably reducing the complexity, but future works will need to undertake the complex task of considering the effect of liquid bridges on realistic non-spherical particles.

7 | CONCLUSIONS

Van der Waals forces, electrostatic forces, and capillary forces are the primary types of cohesive forces that solid particles can experience, causing them to coalesce, stick to one another, and form stable groups of several elements. Although these forces are often neglected by researchers performing simulations of particle–fluid systems, they are always present to some extent and are particularly relevant for certain natural phenomena and industrial applications. In recent years, various studies have been devoted to including these forces in CFD simulations, aimed at reproducing the behaviour of solid particles in multiphase systems, that is, those in which their behaviour is significantly affected by the presence of one or more fluid phases. These simulations have employed different approaches, with varying degrees of detail and computational complexity. In this concise review, we have briefly summarized their main logic and achievements, ascribing them to three main categories: pseudo-single phase approaches, continuum approaches, and discrete element approaches.

Slurries composed of a liquid and low amounts of microscopic solid particles have often been simulated by researchers as a homogeneous phase, employing so-called single-phase approaches. This results in significantly lower computational requirements, but all information on the solid phase is lost and the accuracy can also be hindered. The presence of particles and their cohesiveness affects slurries' viscosity, conferring them a non-Newtonian behaviour. The Hershel–Bulkley, Bingham, or power-law models are the main choices to account for the non-constant viscosity. This approach has especially been employed for sludges in anaerobic digestion and soils in geotechnical applications. With regard to sludges, the effect of the solids concentration and temperature on the rheology is still not ascertained and needs further clarification. Despite these uncertainties, there is ample literature on their simulation and it is nowadays possible to reproduce industrial units.

Continuum-based approaches treat both the solid and the fluid phases as interpenetrating, modelling the former through the kinetic theory of granular flows. This theory was originally developed for cohesionless spherical particles and is hence unsuitable for cohesive particles. To simulate them, researchers have either employed modifications of the kinetic theory of granular flows or only acted on the restitution coefficient, which is a measure of the energy dissipated by colliding particles. Population balance modelling and modified drag correlations are also common to properly account for the presence of particle agglomerates. Continuum-based approaches have been more often applied to particles experiencing van der Waals forces, such as those belonging to Group A of the Geldart classification since it is unfeasible to simulate them through discrete-based methods. Studies on wet particles are instead scarcer. In spite of the various interesting and valuable achievements, these methodologies are still not established, and as such are mostly not included in common

programs employed for such simulations, requiring ad hoc modifications.

Finally, particles can also be simulated as discrete elements, employing the so-called discrete element method (DEM, or CFD-DEM when coupled with fluid dynamic simulations). In it, interparticle forces are directly simulated, so it is also more straightforward to include various types of cohesive forces. Given that simulating realistic systems comprising of micrometric particles is unfeasible even for the most powerful computers, researchers have focused on systems comprising relatively large particles (with sizes of the order of 1 mm) that exhibit a cohesive behaviour due to liquid bridges (most notably, wet fluidized beds). There are many different approaches to account for this effect, with different degrees of accuracy and complexity, and an established one has still not emerged. These simulations may also be employed for small control volume to obtain closure relationships to employ in other less detailed CFD approaches, following a multiscale approach.

As a final observation, already briefly noted in various parts of the review, the lack of adequate experimental data is often a hindrance to the correct and fruitful application of computational techniques. Especially for very fine particles or opaque systems, estimating the magnitude of the cohesive forces may be unfeasible. In this framework, future interdisciplinary efforts that tackle these gaps may be particularly valuable to make these simulations more established.

AUTHOR CONTRIBUTIONS

Filippo Marchelli: Conceptualization; investigation; writing – original draft; methodology; visualization; formal analysis; data curation. **Luca Fiori:** Funding acquisition; writing – review and editing; project administration; resources. **Renzo Di Felice:** Conceptualization; validation; writing – review and editing; supervision.

ACKNOWLEDGEMENTS

The publication was created with the co-financing of the European Union–FSE-REACT-EU, PON Research and Innovation 2014-2020 DM1062/2021.

DATA AVAILABILITY STATEMENT

Data sharing not applicable to this article as no datasets were generated or analyzed during the current study.

REFERENCES

[1] Oxford English Dictionary, "cohesion, n. meanings, etymology and more | Oxford English Dictionary,". https://www.oed.com/dictionary/cohesion_n (accessed: December 2023).
[2] Q. Sun, G. Wang, K. Hu, *Prog. Nat. Sci.* **2009**, *19*, 523.
[3] *Science* **2005**, *309*, 78b.
[4] P. Tahmasebi, *Prog. Mater. Sci.* **2023**, *138*, 101157.
[5] M. Menéndez, J. Herguido, A. Bérard, G. S. Patience, *Can. J. Chem. Eng.* **2019**, *97*, 2383.
[6] W. Zhong, A. Yu, G. Zhou, J. Xie, H. Zhang, *Chem. Eng. Sci.* **2016**, *140*, 16.
[7] H. Ma, L. Zhou, Z. Liu, M. Chen, X. Xia, Y. Zhao, *Powder Technol.* **2022**, *412*, 117972.
[8] C. Q. LaMarche, B. Freireich, R. Cocco, J. W. Chew, *Chem. Eng. J.* **2023**, *471*, 144541.
[9] H. R. Norouzi, S. Golshan, R. Zarghami, *Chem. Prod. Process Model.* **2021**, *17*, 531.
[10] F. Alobaid, N. Almohammed, M. Massoudi Farid, J. May, P. Rößger, A. Richter, B. Epple, *Prog. Energy Combust. Sci.* **2022**, *91*, 100930.
[11] S. Wang, C. Hu, K. Luo, J. Yu, J. Fan, *Particuology* **2023**, *80*, 11.
[12] H. Xu, W. Wang, C. Ma, W. Zhong, A. Yu, *Powder Technol.* **2022**, *409*, 117805.
[13] R. Kamphorst, K. Wu, S. Salameh, G. M. H. Meesters, J. R. van Ommen, *Can. J. Chem. Eng.* **2023**, *101*, 227.
[14] C. M. Boyce, *Powder Technol.* **2018**, *336*, 12.
[15] H. Caillet, L. Adelard, *Waste Biomass Valoriz.* **2023**, *14*, 389.
[16] J. P. K. Seville, C. D. Willett, P. C. Knight, *Powder Technol.* **2000**, *113*, 261.
[17] Q. J. Zheng, R. Y. Yang, Q. H. Zeng, H. P. Zhu, K. J. Dong, A. B. Yu, *Powder Technol.* **2024**, *436*, 119445.
[18] D. Geldart, *Powder Technol.* **1973**, *7*, 285.
[19] R. Cocco, J. W. Chew, *Powder Technol.* **2023**, *428*, 118861.
[20] I. Soleimani, J. Shabanian, J. Chaouki, *Chem. Eng. J.* **2023**, *475*, 146438.
[21] O. B. Adeyinka, S. Samiei, Z. Xu, J. H. Masliyah, *Can. J. Chem. Eng.* **2009**, *87*, 422.
[22] K. L. Johnson, K. Kendall, A. D. Roberts, *Proc. R. Soc. London. A. Math. Phys. Sci.* **1971**, *324*, 301.
[23] F. Raganati, R. Chirone, P. Ammendola, *Chem. Eng. Res. Des.* **2018**, *133*, 347.
[24] Y. Zhao, M. Liu, C.-H. Wang, S. Matsusaka, J. Yao, *Adv. Powder Technol.* **2023**, *34*, 103895.
[25] L. Yang, M. Sega, J. Harting, *AIChE J.* **2021**, *67*, e17350.
[26] H. Xu, W. Zhong, Y. Shao, A. Yu, *Powder Technol.* **2018**, *340*, 26.
[27] C. L. Feng, A. B. Yu, *Powder Technol.* **1998**, *99*, 22.
[28] J. P. Zhang, J. R. Grace, N. Epstein, K. S. Lim, *Chem. Eng. Sci.* **1997**, *52*, 3979.
[29] T. Yehuda, H. Kalman, *Powder Technol.* **2020**, *362*, 288.
[30] G. Alfonsi, *Appl. Mech. Rev.* **2009**, *62*, 04080.
[31] H. Pan, X.-Z. Chen, X.-F. Liang, L.-T. Zhu, Z.-H. Luo, *Powder Technol.* **2016**, *299*, 235.
[32] C. W. Hirt, B. D. Nichols, *J. Comput. Phys.* **1981**, *39*, 201.
[33] A. Ghanbari, Z. Mousavi, M.-C. Heuzey, G. S. Patience, P. J. Carreau, *Can. J. Chem. Eng.* **2020**, *98*, 1456.
[34] M. C. Sadino-Riquelme, A. Donoso-Bravo, F. Zorrilla, E. Valdebenito-Rolack, D. Gómez, F. Hansen, *Chem. Eng. J.* **2023**, *466*, 143180.
[35] L. Li, K. Wang, Q. Zhao, Q. Gao, H. Zhou, J. Jiang, W. Mei, *Rev. Environ. Sci. Bio/Technology* **2022**, *21*, 665.
[36] H. Caillet, A. Bastide, L. Adelard, *Clean. Waste Syst.* **2023**, *6*, 100124.
[37] S. Baroutian, N. Eshtiaghi, D. J. Gapes, *Bioresour. Technol.* **2013**, *140*, 227.

[38] E. Wicklein, D. J. Batstone, J. Ducoste, J. Laurent, A. Griborio, J. Wicks, S. Saunders, R. Samstag, O. Potier, I. Nopens, *Water Sci. Technol.* **2016**, *73*, 969.
[39] C. H. Dang, G. Cappai, J.-W. Chung, C. Jeong, B. Kulli, F. Marchelli, K. S. Ro, S. Román, *Agronomy* **2024**, *14*, 247.
[40] G. Feng, Y. Guo, W. Tan, *Water Sci. Technol.* **2015**, *72*, 2018.
[41] G. Feng, W. Tan, N. Zhong, L. Liu, *Chem. Eng. J.* **2014**, *247*, 223.
[42] X. Cao, Y. Pan, K. Jiang, K. Zhu, X. Ren, *Environ. Technol.* **2021**, *42*, 3707.
[43] F. Marchelli, L. Fiori, *Ind. Eng. Chem. Res.* **2024**, *63*, 4134.
[44] K. J. Craig, M. N. Nieuwoudt, L. J. Niemand, *Water Res.* **2013**, *47*, 4485.
[45] M. Constanza Sadino-Riquelme, J. Rivas, D. Jeison, A. Donoso-Bravo, R. E. Hayes, *Can. J. Chem. Eng.* **2023**, *101*, 6240.
[46] V. Vidal, A. Gay, *Pap. Phys.* **2022**, *14*, 140011.
[47] A. Nermoen, O. Galland, E. Jettestuen, K. Fristad, Y. Podladchikov, H. Svensen, A. Malthe-Srenssen, *J. Geophys. Res. Solid Earth* **2010**, *115*, B10202.
[48] A. Shakeel, A. Kirichek, C. Chassagne, *Geo-Mar. Lett.* **2019**, *39*, 427.
[49] A. Shakeel, A. Kirichek, C. Chassagne, J. Nonnewton, *Fluid Mech.* **2020**, *286*, 104434.
[50] W. Y. Yang, G. L. Yu, S. K. Tan, H. K. Wang, *Int. J. Sediment Res.* **2014**, *29*, 454.
[51] N. Cruz, Y. Peng, *Miner. Eng.* **2016**, *98*, 137.
[52] J. Furlan, R. Visintainer, A. Sellgren, *Can. J. Chem. Eng.* **2016**, *94*, 1108.
[53] H. Alehossein, B. Shen, Z. Qin, C. Huddlestone-Holmes, *J. Mater. Civ. Eng.* **2012**, *24*, 644.
[54] T. L. Chen, L. Y. Zhang, D. L. Zhang, *Comput. Geotech.* **2014**, *58*, 14.
[55] Y.-C. Zhang, D.-D. Pan, D.-Y. Li, Z.-H. Xu, *Acta Geotech.* **2023**, https://doi.org/10.1007/s11440-023-01982-6
[56] T. Wang, B. Song, *Appl. Ocean Res.* **2019**, *82*, 225.
[57] B. Wang, C. van Rhee, A. Nobel, G. Keetels, *Ocean Eng.* **2021**, *227*, 108796.
[58] S. Lovato, A. Kirichek, S. L. Toxopeus, J. W. Settels, G. H. Keetels, *Ocean Eng.* **2022**, *258*, 111632.
[59] N. Gharib, B. Bharathan, L. Amiri, M. McGuinness, F. P. Hassani, A. P. Sasmito, *Can. J. Chem. Eng.* **2017**, *95*, 1181.
[60] S. M. Garimella, M. Ameenuddin, M. Anand, *Can. J. Chem. Eng.* **2023**, *101*, 3624.
[61] A. Rawat, S. N. Singh, V. Seshadri, *Int. J. Coal Prep. Util.* **2022**, *42*, 623.
[62] Z. Wang, W. Guo, W. Ding, K. Liu, W. Qin, C. Wang, Z. Wang, *Powder Technol.* **2023**, *419*, 118375.
[63] L. Wang, L. Cheng, S. Yin, Z. Yan, X. Zhang, *Constr. Build. Mater.* **2023**, *402*, 133014.
[64] D. Carvajal, D. L. Marchisio, S. Bensaid, D. Fino, *Ind. Eng. Chem. Res.* **2012**, *51*, 7518.
[65] D. Wadnerkar, M. Agrawal, M. O. Tade, V. Pareek, *Asia-Pac. J. Chem. Eng.* **2016**, *11*, 467.
[66] D. G. Schaeffer, *J. Differ. Equ.* **1987**, *66*, 19.
[67] D. Gidaspow, R. Bezburuah, J. Ding, presented at Proc. 7th Eng. Foundat. Conf. Fluidizat. **1992**.
[68] M. Syamlal, W. Rogers, T. J. O'Brien, *MFIX Documentation: Volume 1, Theory Guide*, U.S. Department of Energy, Springfield VA **1993**.
[69] C. K. K. Lun, S. B. Savage, D. J. Jeffrey, N. Chepurniy, *J. Fluid Mech.* **1984**, *140*, 223.
[70] J. Wang, *Chem. Eng. Sci.* **2020**, *215*, 115428.
[71] M. Macaulay, P. Rognon, *Soft Matter* **2021**, *17*, 165.
[72] S. Cloete, A. Zaabout, S. T. Johansen, M. van Sint Annaland, F. Gallucci, S. Amini, *Powder Technol.* **2013**, *235*, 735.
[73] W. Wang, B. Lu, N. Zhang, Z. Shi, J. Li, *Int. J. Multiphase Flow* **2010**, *36*, 109.
[74] X. Liu, Y. Shao, W. Zhong, J. R. Grace, N. Epstein, B. Jin, *Can. J. Chem. Eng.* **2013**, *91*, 1800.
[75] F. Q. Mendes, D. Noriler, *Adv. Powder Technol.* **2022**, *33*, 103340.
[76] L. Massaro Sousa, M. C. Ferreira, Q. F. Hou, A. B. Yu, *Powder Technol.* **2019**, *360*, 1055.
[77] H. Movahedi, S. Jamshidi, *J. Pet. Sci. Eng.* **2021**, *198*, 108224.
[78] A. Ibrahim, M. Meguid, *Processes* **2021**, *9*, 785.
[79] Z. Cheng, T.-J. Hsu, J. Calantoni, *Coast. Eng.* **2017**, *119*, 32.
[80] M. Roostaei, A. Nouri, V. Fattahpour, D. Chan, *J. Pet. Sci. Eng.* **2018**, *163*, 119.
[81] A. Ullah, K. Hong, Y. Gao, A. Gungor, M. Zaman, *Renewable Energy* **2019**, *141*, 1054.
[82] T. R. Vakamalla, N. Mangadoddy, *Powder Technol.* **2015**, *277*, 275.
[83] A. Köhler, D. C. Guío-Pérez, A. Prati, M. Larcher, D. Pallarès, *Powder Technol.* **2021**, *393*, 510.
[84] D. C. Guío-Pérez, A. Köhler, A. Prati, D. Pallarès, F. Johnsson, *Can. J. Chem. Eng.* **2023**, *101*, 210.
[85] H. Kim, H. Arastoopour, *Powder Technol.* **2002**, *122*, 83.
[86] L. Huilin, W. Shuyan, Z. Jianxiang, D. Gidaspow, J. Ding, L. Xiang, *Chem. Eng. Sci.* **2010**, *65*, 1462.
[87] B. van Wachem, S. Sasic, *AIChE J.* **2008**, *54*, 9.
[88] M. Ye, J. Wang, M. A. van der Hoef, J. A. M. Kuipers, *Particuology* **2008**, *6*, 540.
[89] L. Wei, Y. Gu, Y. Wang, Y. Lu, *Powder Technol.* **2020**, *364*, 264.
[90] A. H. A. Motlagh, J. R. Grace, M. Salcudean, C. M. Hrenya, *Chem. Eng. Sci.* **2014**, *120*, 22.
[91] C. Luo, W. Zheng, L. Xu, M. Pan, T. Zhou, *Can. J. Chem. Eng.* **2017**, *95*, 1999.
[92] R. I. Jeldres, P. D. Fawell, B. J. Florio, *Powder Technol.* **2018**, *326*, 190.
[93] M. Singh, V. Ranade, O. Shardt, T. Matsoukas, *J. Phys. A: Math. Theor.* **2022**, *55*, 383002.
[94] P. Rajniak, F. Stepanek, K. Dhanasekharan, R. Fan, C. Mancinelli, R. T. Chern, *Powder Technol.* **2009**, *189*, 190.
[95] H. Zhao, A. Maisels, T. Matsoukas, C. Zheng, *Powder Technol.* **2007**, *173*, 38.
[96] M. Vanni, *J. Colloid Interface Sci.* **2000**, *221*, 143.
[97] H. M. Hulburt, S. Katz, *Chem. Eng. Sci.* **1964**, *19*, 555.
[98] R. McGraw, *Aerosol Sci. Technol.* **1997**, *27*, 255.
[99] D. L. Marchisio, R. O. Fox, *J. Aerosol Sci.* **2005**, *36*, 43.
[100] A. K. Thakur, R. Kumar, N. Banerjee, P. Chaudhari, G. K. Gaurav, *Powder Technol.* **2022**, *405*, 117544.
[101] L. Sun, S. Wang, G. Liu, H. Lu, *Chem. Eng. Technol.* **2017**, *40*, 622.
[102] L. Sun, K. Luo, J. Fan, *Chem. Eng. Technol.* **2017**, *40*, 1544.
[103] J. Zheng, Z. Wang, Z. Shen, Z. Wang, Y. Li, H. Zhou, *J. Chem. Eng. Jpn.* **2020**, *53*, 85.
[104] K. M. Kellogg, P. Liu, C. Q. LaMarche, C. M. Hrenya, *J. Fluid Mech.* **2017**, *832*, 345.

[105] K. M. Kellogg, P. Liu, C. M. Hrenya, *Processes* **2023**, *11*, 2553.
[106] K. M. Kellogg, P. Liu, C. M. Hrenya, *Chem. Eng. Sci.* **2019**, *199*, 249.
[107] M. Askarishahi, M.-S. Salehi, S. Radl, *Ind. Eng. Chem. Res.* **2022**, *61*, 3186.
[108] Y. Gu, A. Ozel, J. Kolehmainen, S. Sundaresan, *J. Fluid Mech.* **2019**, *860*, 318.
[109] A. H. Ahmadi Motlagh, K. Pougatch, A. Maturi, M. Salcudean, J. R. Grace, D. Grecov, J. Mcmillan, *Ind. Eng. Chem. Res.* **2019**, *58*, 4396.
[110] H. Zhong, Y. Zhang, Q. Xiong, J. Zhang, Y. Zhu, S. Liang, B. Niu, X. Zhang, *Powder Technol.* **2020**, *364*, 363.
[111] R. H. Davis, D. A. Rager, B. T. Good, *J. Fluid Mech.* **2002**, *468*, 107.
[112] Y. Chen, H. Zhong, R. Tang, J. Zhang, Y. Tian, *Theor. Found. Chem. Eng.* **2023**, *57*, 380.
[113] M. F. Al-Adel, D. A. Saville, S. Sundaresan, *Ind. Eng. Chem. Res.* **2002**, *41*, 6224.
[114] Y. T. Shih, D. Gidaspow, D. Wasan, *AIChE J.* **1987**, *33*, 1322.
[115] R. G. Rokkam, R. O. Fox, M. E. Muhle, *Powder Technol.* **2010**, *203*, 109.
[116] F. Chowdhury, M. Ray, A. Sowinski, P. Mehrani, A. Passalacqua, *Powder Technol.* **2021**, *389*, 104.
[117] H. Grosshans, S. Jantač, *Chem. Eng. J.* **2023**, *455*, 140918.
[118] Y. Liu, H. Wang, Y. Song, H. Qi, *Int. J. Chem. React. Eng.* **2022**, *20*, 357.
[119] B. Blais, D. Vidal, F. Bertrand, G. S. Patience, J. Chaouki, *Can. J. Chem. Eng.* **2019**, *97*, 1964.
[120] P. A. Cundall, O. D. L. Strack, *Géotechnique* **1979**, *29*, 47.
[121] A. Bérard, G. S. Patience, B. Blais, *Can. J. Chem. Eng.* **2020**, *98*, 424.
[122] C. M. Boyce, D. J. Holland, S. A. Scott, J. S. Dennis, *Ind. Eng. Chem. Res.* **2015**, *54*, 10684.
[123] E. Butaye, A. Toutant, S. Mer, F. Bataille, *Comput. Fluids* **2023**, *267*, 106071.
[124] H. P. Zhu, Z. Y. Zhou, R. Y. Yang, A. B. Yu, *Chem. Eng. Sci.* **2008**, *63*, 5728.
[125] F. Marchelli, R. Di Felice, *Chem. Eng. Trans.* **2021**, *86*, 811.
[126] M. Lungu, J. Siame, L. Mukosha, *Powder Technol.* **2021**, *378*, 85.
[127] C. Moliner, F. Marchelli, N. Spanachi, A. Martinez-Felipe, B. Bosio, E. Arato, *Chem. Eng. J.* **2019**, *377*, 120466.
[128] A. Di Renzo, E. Napolitano, F. Di Maio, *Processes* **2021**, *9*, 279.
[129] D. Kazidenov, F. Khamitov, Y. Amanbek, *Gas Sci. Eng.* **2023**, *113*, 204976.
[130] J. Tausendschön, J. Kolehmainen, S. Sundaresan, S. Radl, *Powder Technol.* **2020**, *364*, 167.
[131] A. Stroh, F. Alobaid, M. T. Hasenzahl, J. Hilz, J. Ströhle, B. Epple, *Particuology* **2016**, *29*, 34.
[132] P. Kieckhefen, S. Pietsch, M. Dosta, S. Heinrich, *Annu. Rev. Chem. Biomol. Eng.* **2020**, *11*, 397.
[133] Z. Zhao, L. Zhou, L. Bai, B. Wang, R. Agarwal, *Arch. Comput. Methods Eng.* **2024**, *31*, 871.
[134] Z. Rahimi-Ahar, M. S. Hatamipour, *Rev. Chem. Eng.* **2018**, *1*, 25.
[135] C. Moliner, F. Marchelli, B. Bosio, E. Arato, *Energies* **2017**, *10*, 38.
[136] K. W. Chu, B. Wang, D. L. Xu, Y. X. Chen, A. B. Yu, *Chem. Eng. Sci.* **2011**, *66*, 834.
[137] D. D. Attanayake, F. Sewerin, S. Kulkarni, A. Dernbecher, A. Dieguez-Alonso, B. van Wachem, *Flow, Turbul. Combust.* **2023**, *111*, 355.
[138] D. E. P. Zhou, S. Guo, J. Zeng, Q. Xu, L. Guo, Q. Hou, A. Yu, *Fuel* **2022**, *311*, 122490.
[139] J. Capecelatro, W. Longest, C. Boerman, M. Sulaiman, S. Sundaresan, *Adv. Drug Delivery Rev.* **2022**, *188*, 114461.
[140] Y. Guo, X. (Bill) Yu, *Int. J. Multiph. Flow* **2017**, *91*, 89.
[141] F. Geng, J. An, Y. Wang, C. Gui, H. Guo, T. Wen, *Environ. Sci. Pollut. Res.* **2023**, *30*, 102244.
[142] Y.-B. Choi, R.-W. Kim, I. Lee, *Biosyst. Eng.* **2024**, *237*, 196.
[143] J. Sun, X.-A. Li, J. Li, J. Zhang, Y. Zhang, *Catena* **2023**, *222*, 106729.
[144] X. Bao, H. Wu, H. Xiong, X. Chen, *Ocean Eng.* **2023**, *284*, 115140.
[145] A. Haghnegahdar, R. Bharadwaj, Y. Feng, *Powder Technol.* **2023**, *427*, 118710.
[146] C. Porcaro, M. Saeedipour, *Comput. Methods Programs Biomed.* **2023**, *231*, 107400.
[147] A. N. Balachandran Nair, S. Pirker, M. Saeedipour, *Comput. Part. Mech* **2022**, *9*, 759.
[148] M. Ebrahimi, S. Thakur, C. J. Coetzee, O. C. Scheffler, *Process* **2022**, *11*, 5.
[149] J. K. Pandit, X. S. Wang, M. J. Rhodes, *Powder Technol.* **2006**, *164*, 130.
[150] M. Rhodes, X. Wang, M. Nguyen, P. Stewart, K. Liffman, *Chem. Eng. Sci.* **2001**, *56*, 4433.
[151] H. Fan, D. Mei, F. Tian, X. Cui, M. Zhang, *Powder Technol.* **2016**, *288*, 228.
[152] T. Kobayashi, T. Tanaka, N. Shimada, T. Kawaguchi, *Powder Technol.* **2013**, *248*, 143.
[153] M. Ye, M. van der Hoef, J. A. Kuipers, *Powder Technol.* **2004**, *139*, 129.
[154] R. Moreno-Atanasio, B. H. Xu, M. Ghadiri, *Chem. Eng. Sci.* **2007**, *62*, 184.
[155] J. E. Galvin, S. Benyahia, *AIChE J.* **2014**, *60*, 473.
[156] T. Li, S. Rabha, V. Verma, J.-F. Dietiker, Y. Xu, L. Lu, W. Rogers, B. Gopalan, G. Breault, J. Tucker, R. Panday, *Adv. Powder Technol.* **2017**, *28*, 2961.
[157] P. Liu, C. Q. LaMarche, K. M. Kellogg, C. M. Hrenya, *Chem. Eng. Sci.* **2016**, *145*, 266.
[158] Q. F. Hou, Z. Y. Zhou, A. B. Yu, *Chem. Eng. Sci.* **2012**, *84*, 449.
[159] Y. Wu, Q. Hou, A. Yu, *AIChE J.* **2020**, *66*, e16944.
[160] P. Breuninger, D. Weis, I. Behrendt, P. Grohn, F. Krull, S. Antonyuk, *Particuology* **2019**, *42*, 114.
[161] Y. Zou, R. Zou, Y. Wu, *Powder Technol.* **2024**, *436*, 119512.
[162] N. Almohammed, M. Breuer, *Powder Technol.* **2016**, *294*, 373.
[163] O. L. Sgrott, M. Sommerfeld, *Can. J. Chem. Eng.* **2019**, *97*, 511.
[164] M. Sommerfeld, Y. Cui, S. Schmalfuß, *Eur. J. Pharm. Sci.* **2019**, *128*, 299.
[165] Y. Song, T. Zhou, R. Bai, M. Zhang, H. Yang, *Processes* **2023**, *11*, 382.
[166] H. Xu, W. Zhong, Z. Yuan, A. B. Yu, *Powder Technol.* **2017**, *314*, 377.

[167] T. Mikami, H. Kamiya, M. Horio, *Chem. Eng. Sci.* **1998**, *53*, 1927.
[168] P. Y. Liu, R. Y. Yang, A. B. Yu, *Chem. Eng. Sci.* **2013**, *86*, 99.
[169] Y. He, W. Peng, T. Wang, S. Yan, *Math. Probl. Eng.* **2014**, *2014*, 1.
[170] R. R. Zhu, W. B. Zhu, L. C. Xing, Q. Q. Sun, *Powder Technol.* **2011**, *210*, 73.
[171] M. Wu, J. G. Khinast, S. Radl, *AIChE J.* **2018**, *64*, 437.
[172] R. Lu, L. Zhang, P. Ricoux, L. Wang, *Powder Technol.* **2019**, *356*, 222.
[173] X. Wang, M. Rhodes, *Chem. Eng. Sci.* **2004**, *59*, 215.
[174] Z. Mansourpour, N. Mostoufi, R. Sotudeh-Gharebagh, *Can. J. Chem. Eng.* **2013**, *91*, 560.
[175] A. Deng, T. Tang, S. Sun, Y. He, *Chem. Eng. J.* **2023**, *476*, 146480.
[176] Y. Zhou, H. Li, M. Zhu, X. Hu, H. Yuan, S. Jiang, L. Han, *Chem. Eng. Process. Process Intensif.* **2020**, *153*, 107928.
[177] E. L. Chan, K. Washino, *Chem. Eng. Res. Des.* **2018**, *132*, 1060.
[178] M. S. van Buijtenen, N. G. Deen, S. Heinrich, S. Antonyuk, J. A. M. Kuipers, *Can. J. Chem. Eng.* **2009**, *87*, 308.
[179] P. Darabi, K. Pougatch, M. Salcudean, D. Grecov, *Powder Technol.* **2011**, *214*, 365.
[180] P. Darabi, K. Pougatch, M. Salcudean, D. Grecov, *Chem. Eng. Sci.* **2009**, *64*, 1868.
[181] C. Song, D. Liu, J. Ma, X. Chen, *Powder Technol.* **2017**, *314*, 346.
[182] V. S. Sutkar, N. G. Deen, J. T. Padding, J. A. M. Kuipers, V. Salikov, B. Crüger, S. Antonyuk, S. Heinrich, *AIChE J.* **2015**, *61*, 769.
[183] V. S. Sutkar, N. G. Deen, A. V. Patil, V. Salikov, S. Antonyuk, S. Heinrich, J. A. M. Kuipers, *Chem. Eng. J.* **2016**, *288*, 185.
[184] N. Saparbayeva, Y. F. Chang, P. Kosinski, A. C. Hoffmann, B. V. Balakin, P. G. Struchalin, *Powder Technol.* **2023**, *426*, 118660.
[185] N. Saparbayeva, B. V. Balakin, *Sci. Rep.* **2023**, *13*, 17188.
[186] S. Watano, S. Saito, T. Suzuki, *Powder Technol.* **2003**, *135–136*, 112.
[187] C. Pei, C.-Y. Wu, D. England, S. Byard, H. Berchtold, M. Adams, *Powder Technol.* **2013**, *248*, 34.
[188] M. W. Korevaar, J. T. Padding, M. A. Van der Hoef, J. A. M. Kuipers, *Powder Technol.* **2014**, *258*, 144.
[189] J. Kolehmainen, A. Ozel, C. M. Boyce, S. Sundaresan, *AIChE J.* **2017**, *63*, 1872.
[190] M. A. Hassani, R. Zarghami, H. R. Norouzi, N. Mostoufi, *Powder Technol.* **2013**, *246*, 16.
[191] J. Kolehmainen, A. Ozel, C. M. Boyce, S. Sundaresan, *AIChE J.* **2016**, *62*, 2282.
[192] C. Wang, G. Liu, Z. Zhai, X. Guo, Y. Wu, *Powder Technol.* **2023**, *419*, 118340.
[193] F. O. Alfano, A. Di Renzo, F. P. Di Maio, M. Ghadiri, *Powder Technol.* **2021**, *382*, 491.

How to cite this article: F. Marchelli, L. Fiori, R. Di Felice, *Can. J. Chem. Eng.* **2024**, 1. https://doi.org/10.1002/cjce.25269